

1
NASA TECHNICAL TRANSLATION

NASA TT F-15,213

CALCULATION OF POTENTIAL FLOW ABOUT AXIALLY SYMMETRIC FUSELAGES,
ANNULAR PROFILES AND ENGINE INLETS

W. Geissler

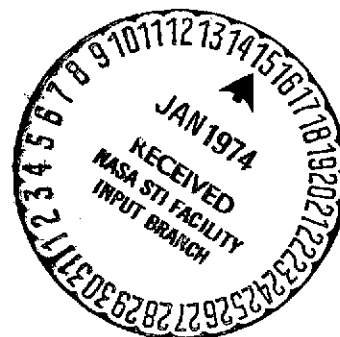
Translation of "Berechnung der Potentialströmung um rotations-
symmetrische Rümpfe, Ringprofile und Treibwerkseinläufe,"
Zeitschrift für Flugwissenschaften, Vol. 20, No. 12,
December 1972, pp. 457-462

(NASA-TT-F-15213) CALCULATION OF
POTENTIAL FLOW ABOUT AXIALLY SYMMETRIC
FUSELAGES, ANNULAR PROFILES AND ENGINE
INLETS (Kanner (Leo) Associates), 74 p
HC \$3.00

N74-13707

Unclas

CSCL 01A G3/01 25366



NATIONAL AERONAUTICS AND SPACE ADMINISTRATION
WASHINGTON, D.C. 20546
DECEMBER 1973

1. Report No. NASA TT F-15,213	2. Government Accession No.	3. Recipient's Catalog No.	
4. Title and Subtitle CALCULATION OF POTENTIAL FLOW ABOUT AXIALLY SYMMETRIC FUSELAGES, ANNULAR PROFILES AND ENGINE INLETS		5. Report Date December 1973	
		6. Performing Organization Code	
7. Author(s) W. Geissler		8. Performing Organization Report No.	
		10. Work Unit No.	
9. Performing Organization Name and Address Leo Kanner Associates Redwood City, California 94063		11. Contract or Grant No. NASw-2481	
		13. Type of Report and Period Covered Translation	
12. Sponsoring Agency Name and Address National Aeronautics and Space Administration, Washington, D.C. 20546		14. Sponsoring Agency Code	
15. Supplementary Notes Translation of "Berechnung der Potentialströmung um rotations-symmetrische Rumpfe, Ringprofile und Triebwerkseinläufe," Zeitschrift für Flugwissenschaften, Vol. 20, No. 12, December 1972, pp. 457-462			
16. Abstract The calculation of the potential flow about bodies of revolution (closed bodies, inlets, cowls) is done by a method using surface distributions of sources, sinks and vortices. This method deals with the case of an arbitrary flow about the body. Besides axisymmetric flows and flows at incidence to the body axis it is possible to take care of the flow field induced by another body (interference problem). A panel method is used for the numerical solution of the problem. In the case of an axisymmetric body, the surface elements are frustums of cones of small axial length. For different types of bodies the results of this method are compared with measurements.			
17. Key Words (Selected by Author(s))		18. Distribution Statement Unclassified-Unlimited	
19. Security Classif. (of this report) Unclassified	20. Security Classif. (of this page) Unclassified	21. No. of Pages 15	22. Price

CALCULATION OF POTENTIAL FLOW ABOUT AXIALLY SYMMETRIC FUSELAGES, ANNULAR PROFILES AND ENGINE INLETS

W. Geissler

Aerodynamische Versuchsanstalt Göttingen der Deutschen
Forschungs- und Versuchsanstalt für Luft- und Raumfahrt (DFVLR).

1. Introduction

/457*

A numerical method of calculation is given by A.M.O. Smith and J. Pierce [1] for determining potential flow about axially symmetric bodies which makes use of a surface distribution of source-sink rings. While the case of oncoming flow parallel to the axis is covered in [1], J. L. Hess [2] treats bodies of revolution in transverse flow. A pure source-sink distribution is not adequate for the special case of an annular profile. It was shown in [3] that an additional circulation is necessary in order to satisfy Kutta's flowoff condition at the trailing edge of the annular profile. This circulation is likewise applied to the profile surface in [3] as a ring-vortex distribution of constant vorticity.

An expanded theory is presented in the following article which covers the case of an annular profile or body of revolution in a more general form of oncoming flow (parallel flow which is parallel or oblique to the axis; interference effects). To solve this problem, Smith and Pierce's method of surface distribution (panel method) is combined with a formulation by F. W. Riegels [4] and J. Weissinger [6] for the variation in flow parameters in the tangential direction.

* Numbers in the margin indicate pagination in the foreign text.

The general method for annular profiles, with suitable simplifications, is also made applicable to power plant inlets and axially symmetrical fuselages.

2. Notation

2.1. Geometric Quantities

x, r, ϕ	Cylindrical coordinates (position of plotted point)
x', r', ϕ'	Position of surface covered
R_0	Reference radius
r_i	Inside radius
r_h	Hub radius
L	Reference length
D	Diameter
α	Angle of attack (angle between axis of body of revolution and oncoming-flow direction)

2.2. Aerodynamic Quantities

/458

V	Oncoming-flow velocity
v	Induced velocity of system of singularities
γ	Vortex density
q	Source density
p	Static pressure
p_∞	Pressure in undisturbed flow
q_∞	Stagnation pressure [= $(\rho/2)V^2$]
c_p	Pressure coefficient [= $(p - p_\infty)/q_\infty$]

ζ	Flow index	$\left[= \frac{2}{r_h^2} \int_{r_h}^{r_R} r \frac{v_r(r)}{V} dr \right]$
---------	------------	---

2.3. Subscripts

∞	Oncoming flow
x	Axial

r	Radial
ϕ	Tangential direction
γ	Vortex distribution
q	Source distribution
N	Normal to section contour
i	Point plotted
j	Position of surface covered
h	Hub
iR	Inside radius of annular contour

3. Problem; System of Singularities

The recalculation problem, the so-called second principle problem of the profile theory, will be solved for bodies of revolution. The geometry of the body and the form of oncoming flow are assumed to be known. Since interference effects must be taken into consideration, in addition to parallel oncoming flows, the disturbing body must also be represented by singularities.

Fig. 1 shows the system of singularities employed, exemplified by an annulus section with a hub body. The cases of a fuselage and a power plant inlet with varying flow through it can be derived from this by suitable simplification of the vortex system.

In Fig. 1, the surface of the annulus section and of the hub body are covered with a continuous ring-source distribution. A ring-vortex distribution (bound vortices) which is constant in the axial direction lies on the surface of the annular profile, so that Kutta's flowoff condition (smooth flowoff) is satisfied at the trailing edge of the section. If the intensity of these bound vortices changes in the tangential direction ϕ of the profile, then, according to Helmholtz's third theorem of vortices, free vortices must leave which follow the lines of flow. These free vortices are assumed to travel along the profile contour in

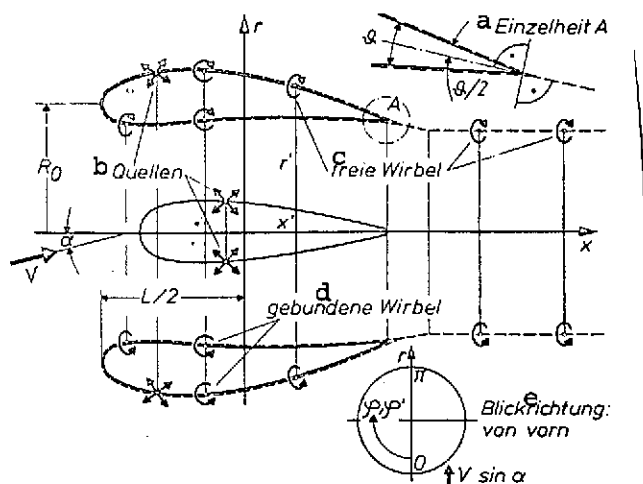


Fig. 1. Annulus section with hub, system of singularities.

Key: a. Detail A; b. Sources; c. Free vortices; d. Bound vortices; e. Viewed from upstream

singularities of equal magnitude and opposite direction:

$$v_q N_i = V_{N_i} + v_\gamma N_i \quad (\text{at plotted point } i) \quad (1)$$

In equation (1), the normal velocity of the entire vortex system $v_\gamma N_i$ has been placed on the right side of the equation along with the normal oncoming-flow component V_{N_i} . Vortex strength γ , which is contained in $v_\gamma N_i$, is first arbitrarily set equal to 1, for example. Vortex strength is not calculated until later, with the aid of Kutta's flowoff condition. The normal components of the two terms on the right side of (1) must be compensated for by suitable source distributions $q(x, \phi)$.

Velocity components v_q and v_γ are calculated with the aid of the Biot-Savart law. Equation (1) thus yields a two-dimensional (x - and ϕ -dependent) integral equation for determining the unknown source distribution q which is contained in $v_q N$. This

meridional sections and are laid on a semi-infinite vortex cylinder parallel with the axis behind the profile.

4. Formulae, Numerical Solution

Calculation is centered around the kinematic flow condition: The normal components induced at the position of the body of revolution by the external oncoming flow must be compensated for by a normal component of the system of

two-dimensional integral equation can, according to F. W. Riegels [4] and J. Weissinger [6], be transformed into a sum of one-dimensional (x-dependent, only) integral equations by means of Fourier series for V_N and for source strength q and vortex strength γ . With

$$V_N(x', \varphi') = V \sum_{n=0}^{\infty} c_n(x') \cos n \varphi', \quad (2)$$

$$q(x', \varphi') = V \sum_{n=0}^{\infty} g_{qn}(x') \cos n \varphi', \quad (3)$$

$$\gamma(x', \varphi') = V \sum_{n=0}^{\infty} g_{\gamma n}(x') \cos n \varphi' \quad (4)$$

(1) is transformed to

$$V \sum_{j=1}^m [(g_{q\infty j} + g_{q\gamma j}) N_{qj}] = 2\pi V (g_{q\infty i} + g_{q\gamma i}) = V N_i + v_{\gamma N_i} \quad (i = 1, 2, \dots, m). \quad (5)$$

Equation (5) applies to each oncoming-flow case n .

In (5), $g_{q\infty j}$ represents the source strength sought for the compensation of V_{Ni} ; $g_{q\gamma j}$ compensates for the resultant normal component of the vortex system ($v_{\gamma N}$). The particular advantage in using expressions (2) through (4) is that the dependence upon tangential angle ϕ is eliminated in equation (5). A single-dimensional (x-dependent, only) system of equations thus remains in which $n = 0, 1, 2, \dots$ each represent a specific oncoming-flow case. /459

In the form of (5), we already have the kinematic flow condition as a linear system of equations with two terms on the right. In the panel method described by J. L. Hess [2], the surface of the body of revolution is divided into conic frustums of small axial extension, distributed as uniformly as possible. The kinematic flow

condition is satisfied at the center of the surface of each such conic frustum. In (5), N_{qij} indicates the effect of frustum j , covered with source rings, at plotted point i . The sum of normal components of all m -intervals yields the resultant normal component at point i .

Solution of the system of linear equations (5) now yields amplification factors $g_{q\infty j}$, $g_{q\gamma j}$ for each case of oncoming flow n . The associated tangential velocities at the surface of the body can thereby be calculated. The sum of tangential velocities from all cases of oncoming flow finally yields resultant velocity for calculating the pressure distribution.

The "influence function" N_q and the resultant normal velocity of the overall vortex system $v_{\gamma N}$ are determined in a complex manner by the geometry of the body of revolution. These functions will not be described in detail here.

The dependence of the functions upon tangential direction ϕ can always be reduced to integrals of the form

$$G_n(k^2) = (-1)^n \int_0^{\pi/2} \frac{\cos 2n\psi}{(1 - k^2 \sin^2 \psi)^{3/2}} d\psi \quad (6)$$

where

$$k^2 = \frac{4rr'}{(x-x')^2 + (r+r')^2}, \quad \varphi' - \varphi = \pi - 2\psi$$

These functions have been presented and tabulated by F. W. Riegels [4, 5]. The subscript n in (6) is identical to the subscript n in Fourier series (2) through (4). These G functions are constructed recursively from the complete elliptic integrals of the first and second types and are particularly well suited to numerical calculation.

5. Examples of Applications

5.1. Axially Symmetrical Fuselages

The method initially described for annular profiles can be likewise applied to closed axially symmetrical fuselages, with simplification. The assumption is made, however, that the fuselage possesses no lift. A pure source-sink distribution on the surface of the body is then sufficient, and the kinematic flow condition (1) is simplified to

$$v_{q \ Nl} = V_{Nl}. \quad (7)$$

Thus systems of linear equations are produced with only one term on the right side in each case, and each result is just a solution vector $g_{q \infty j}$.

In the case that the freestream is parallel to the axis has already been studied in detail in [3] for various fuselage-type bodies.

Fig. 2 shows calculated pressure distributions for different meridional sections ($\phi = 0^\circ, 60^\circ, 180^\circ$) of a body of revolution, in oblique oncoming flow, which converges to a point in front and becomes a cylindrical shaft downstream. In the case of oblique oncoming flow, only the first two terms ($n = 0$ and 1) are required in series (2) through (4).

The calculations have been compared with measurements made in the transonic wind tunnel at AVA Göttingen by E. Wedemeyer. In the upstream region of the body, the discrepancy between theory and measurement is slight and is caused by the Mach number effect. Only in the $x/L = 1$ region do the deviations become larger at $\phi = 180^\circ$. Paint patterns indicate that a local separation "bubble" occurs in this area.

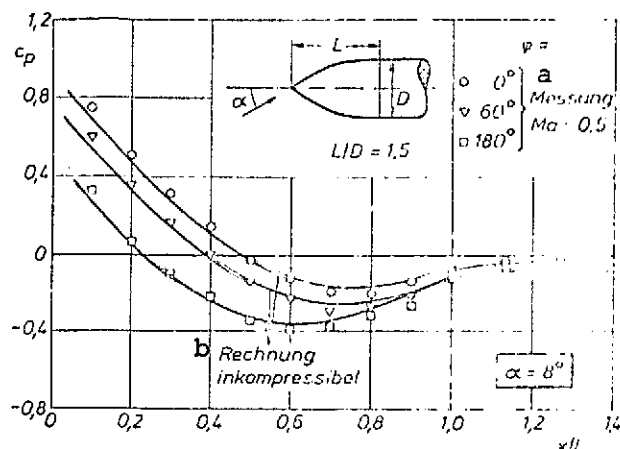


Fig. 2. Fuselage in oblique freestream.

Key: a. Measured data;
b. Calculated data; incompressible.

strength is assumed here in the tangential direction on this body of revolution ($n = 0$ in series (4)). Vortex strength is determined with the aid of mass throughflow.

The dimensionless throughflow index is defined as

$$\zeta = \frac{2}{r_{ik}^2} \int_{r_h}^{r_R} r \frac{v_x(r)}{V} dr \quad (8)$$

where $v_x(r)$ is resultant axial velocity in the internal cross section, composed of the effect of the system of singularities and an external freestream component. Using the panel method makes it possible to write formula (8) as a formula of sums and to solve it with respect to circulation strength γ , and thus to calculate the associated γ for a given mass throughflow.

A power plant inlet with a hub body is outlined in Fig. 3 on which measurements were performed at the AVA Göttingen during the 1940s by D. Küchemann and J. Weber [7]. The comparative experimental results have been taken from that report.

5.2. Power Plant Inlets

Power plant inlets are some other configurations to which the method described can be applied. The upstream portion of an annular profile is involved here whose contours extend downstream in cylindrical form. The system of singularities outlined in Fig. 1 is used, but without free vortices. For simplification, only a constant vortex

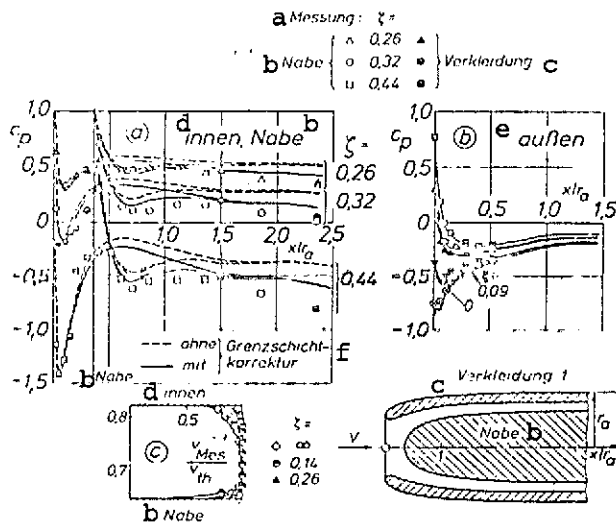


Fig. 3. Cowl 1 with hub, $\alpha = 0^\circ$, with boundary layer correction.

Key: a. Measured data; b. Hub; c. Cowl; d. Inside; e. Outside; f. Without/with boundary layer correction.

Fig. 3 a shows pressure distribution on the internal contour and hub. Pressure distributions on the external contour of the inlet are shown in Fig. 3 b. Fig. 3 c contains measured velocity distributions over the internal cross section of the cylindrical portion. The parameter in each case is throughflow index ζ as defined in (8), assumed to have equal measured and theoretical values. /460

The results of calculations without friction are first plotted in Fig. 3 as dashed curves. Pronounced deviations from the measured values are observed, particularly in the rear inlet section. Better agreement can be obtained with the following boundary layer correction: the results from the potential theory calculation serve as input for a boundary layer program [8]. The displacement thickness of the boundary layer is determined from the boundary layer calculation and is added to the body contour. A second potential theory calculation is carried out for the same throughflow coefficient ζ for the body contour which has been modified in this manner. The results of this calculation are shown as solid curves in Fig. 3 a: They are distinctly closer to the measured values.

In the measurements, however, an additional acceleration of the internal flow is caused by a separation bubble which occurs downstream from the pronounced pressure minimum on the internal

contour and which results in an additional displacement. We find this separation blister to be a region of reduced velocity in the measured velocity distribution in Fig. 3 c. The effect of the boundary layer upon pressure distribution on the external contour (Fig. 3 b) is only very slight.

Fig. 4 shows the same inlet contour in an oblique freestream ($\alpha = 10^\circ$). Here, excellent agreement with the measured data is found on the outside. Separation is clearly evident on the inside at the pressure minimum (at $\phi = 0^\circ$). Thus agreement is not so good in the rear inlet section, due to boundary layer effects. No boundary layer correction was undertaken here.

5.3. Stationary Inlets

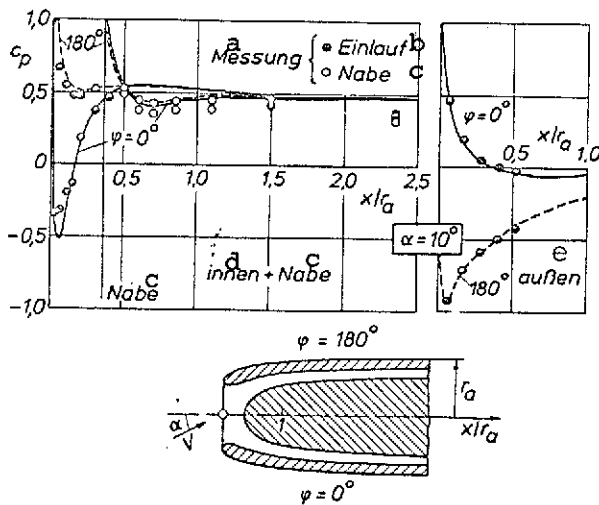


Fig. 4. Cowl 1 with hub in oblique oncoming flow, $\zeta = 0.28$.

Key: a. Measured data; b. Inlet; c. Hub; d. Inside; e. Outside

The stationary inlet represents an extreme case in which a clean flow to the compressor of a power plant must still be guaranteed. No external oncoming flow exists here. Calculation is simplified so that the kinematic flow condition (2) contains only one term on the right:

$$v_q N_i = v_\gamma N_i \quad (9)$$

Only the normal components of the constant circulation distribution must be compensated for by a suitable source distribution.

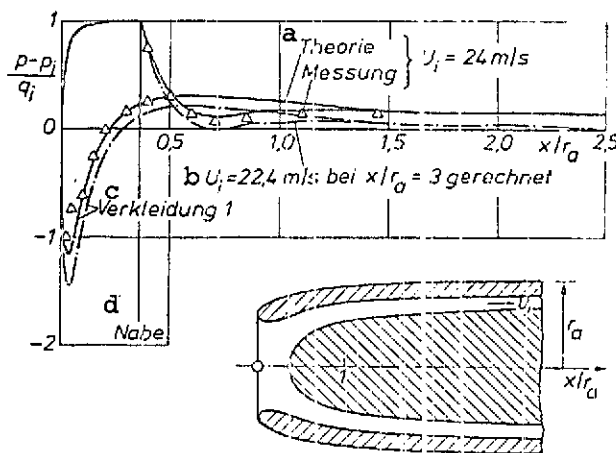


Fig. 5. Cowl 1 with hub, stationary.

Key: a. Theorie / measured data;
b. $U_i = 22.4$ m/s calculated at
 $x/r_a = 3$; c. Cowl; d. Hub.

nounced. If we use the reference velocity determined by measurement (24 m/sec), we obtain good agreement between measurement and theory.

5.4. Annular Profiles of Finite Length

Pressure distributions about three axially symmetric annular profiles with central bodies have already been calculated in [3] and compared with measurements made in the Royal Aircraft Establishment in England [9]. The case of oblique oncoming flow will be studied in the following.

The entire system of singularities shown in Fig. 1 is required for this problem, including the system of free vortices. Again, the first two terms $n = 0$ and 1 are to be used in series (2) through (4) for an oblique freestream.

The inlet contour described above is studied for the stationary case and compared with measured data in Fig. 5. Values in the cylindrical inlet portion serve as reference quantities. The reference velocity determined from potential theory (22.4 m/sec) proves to be too small, due to acceleration caused by the boundary layer. The pressure minimum (dashed curve) is too highly pro-

Fig. 6 contains calculated pressure distributions and those measured in the RAE¹ on an annular profile with a central body at a 5° angle of attack. Agreement between measurement and theory is quite satisfactory in all sections studied. Relatively large deviations are observed in the downstream inside portion of the annular profile. Again, this may possibly involve an acceleration of flow by the effect of the boundary layer at the internal contour and hub body (see Section 5.2).

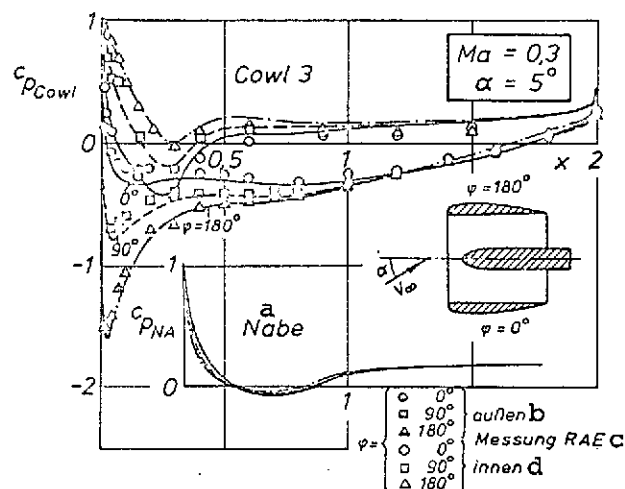


Fig. 6. Annular profile in oblique freestream (cowl 3), $\alpha = 5^\circ$.

Key: a. Hub; b. Outside;
c. Measured data RAE; d. Inside

6. Bodies of Revolution in the Fields of Disturbing Bodies (Interference Problem)

Until now, bodies of revolution have only been studied in parallel flows. For these cases, the term $n = 0$ (parallel to axis) or the terms $n = 0$ and 1 (oblique to axis) were sufficient in series (2). If the effect of a disturbing body in the vicinity of the body of revolution is to be taken into consideration, we need additional terms in the

Fourier series, and thereby obtain a correspondingly higher number of systems of linear equations (5). The condition is that the disturbing body can also be represented by a system of singularities.

Interference calculations can be carried out iteratively: The calculations are first made for the body of revolution and the

¹ These experimental results have generously been made available to me by Messrs. J. A. Bagley and C. Young.

disturbing body, separately, in the associated parallel flow (zeroth approximation). The effect of the source vortex strengths, as determined from the zeroth approximation, upon the neighboring body is then determined, and again source vortex strengths to compensate for these effects are calculated here (first approximation). This can be followed by a second and third approximation. Experience shows that it is possible to stop at just the second approximation with sufficient accuracy.

6.1. Annular Profile Near the Ground

An annular profile (without central body) close to the ground was studied at two different heights above the latter as an important example of such an interference calculation (Fig. 7). The effect of the ground can be simulated in accordance with the reflection principle by a second annular profile at twice the distance of the ground. In this case, the disturbing body is thus again an annular profile. For this problem it is sufficient to consider the first six cases of oncoming flow, $n = 0, 1, \dots, 5$.

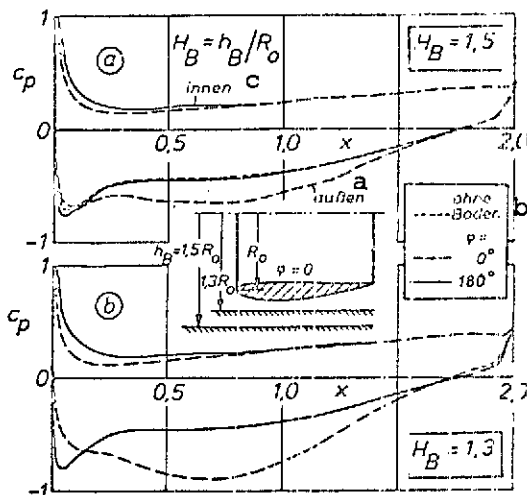


Fig. 7. Annular section (cowling) with ground.

Key: a. Outside; b. Without ground; c. Inside

This method can be used to treat a whole series of additional interference problems, a few of which might be mentioned here: Interference between an annular profile and a fuselage; two annular profiles in a bypass arrangement (with and without oblique flow); interferences between an annular profile and a symmetrical wing.

7. Summary

A method of singularities has been given for calculating potential flow about bodies of revolution. The bodies of revolution here can be in a general form of oncoming flow, i.e. besides parallel flows (parallel to the axis or oblique to the axis), it is also possible to take interference effects caused by disturbing bodies into consideration. For the three-dimensional normal component distribution which occurs on the body of revolution, as in the case of the source-sink and vortex distributions, a Fourier series is set up for the compensation of these normal components. The use of this series makes it possible to transform the kinematic flow condition, which initially appears as a two-dimensional (x - and ϕ -dependent) integral equation, into a sum of one-dimensional (x -dependent, only) integral equations, which can be solved separately with the aid of linear equations, via a panel method.

It has been shown that the method can be applied both to closed fuselage contours (without lift, however) and to power plant inlets with and without oncoming flow and annular profiles of finite length. The computed potential flow results agree well with the measured data.

REFERENCES

1. Smith, A. M. O. and Pierce, J., "Exact solution of the Neumann problem," Douglas Rep. 26, 988 (1958).
2. Hess, J. L., "Calculation of potential flow about bodies of revolution having axis perpendicular to the freestream direction," Douglas Rep. 29, 812 (1960).
3. Geissler, W., "Calculation of potential flow about axially symmetrical angular profiles," dissertation, Braunschweig Engineering University, 1970. Mitteilungen aus dem Max-Planck-Institut für Strömungsforschung und der Aerodynamischen Versuchsanstalt Göttingen, No. 47, 1970. An abbreviated version is being published in Z. Flugwiss. 21(1) (1973). /462
4. Riegels, F. W., "Flow about slender, almost axially symmetrical bodies," Mitteilungen aus dem Max-Planck-Institut für Strömungsforschung, Göttingen, No. 5, 1952.
5. Riegels, F. W., "Formulas and tables for an elliptic integral occurring in three-dimensional potential theory," Arch. Math. 1, 117-125 (1949).
6. Weissinger, J., "The aerodynamics of the annular airfoil in incompressible flow," Z. Flugwiss. 4, 141-150 (1956).
7. Küchemann, D., and Weber, J., "Flow about annular cowls. Fourth Report: Wind tunnel measurements performed on inlet equipment," AVA Report 41/1/12, 1941.
8. Rotta, J. C., "FORTRAN IV computer program for boundary layers in compressible, plane, axially symmetrical flows," Deutsche Luft- und Raumfahrt, FB 71-51, 1971.
9. Young, C., "An investigation of annular aerofoils for turbofan engine cowls," RAE Techn. Rep. 69,205, 1969.